Journal of Materials Chemistry B

RSC Publishing

PAPER

View Article Online
View Journal | View Issue

Cite this: *J. Mater. Chem. B*, 2013, **1**, 3950

Multifunctional graphene magnetic nanosheet decorated with chitosan for highly sensitive detection of pathogenic bacteria†

Hani Nasser Abdelhamid[a] and Hui-Fen Wu*[abcd]

Received 24th March 2013
Accepted 21st May 2013

DOI: 10.1039/c3tb20413h

www.rsc.org/MaterialsB

Multifunctional graphene magnetic nanosheet decorated with chitosan (GMCS) is demonstrated as a promising biosensor for fluorescence spectroscopy and it can be also applied for matrix assisted laser desorption/ionization mass spectrometry (MALDI-MS) for sensitive pathogenic bacteria detection. Graphene-magnetic@chitosan (GMCS) can be applied for multiple applications such as fluorescence biosensor, fluorescence background suppressor, acting as co-matrix, enriching nanoprobe, and separation by external magnets for pathogenic bacteria (*Pseudomonas aeruginosa* and *Staphylococcus aureus*) present in aqueous suspension or blood colloids. GMCS has been prepared and characterized using various techniques including TEM, UV, FTIR, XRD, Raman and fluorescence spectroscopy. Due to the non-covalent interactions among the pathogenic bacteria with the GMCS, fluorescence enhancement takes place as a function of bacterial cell number with a low number of cell detection (4.5×10^2 to 5.0×10^2 cfu mL^{-1}) and wide linear dynamic range which indicates that the GMCS approach is an excellent quantitative methodology and highly sensitive approach for detection of bacteria cells. Graphene works intrinsically as a fluorescence quencher for blood fluorophores and cell autofluorescence as graphene typically has a long life time, which allows detection of the bacteria signals by direct fluorescence measurements. Because of the high fluorescence enhancement efficiency, and large surface area (to volume ratio) of graphene, GMCS exhibits extraordinarily high sensitivity for complex (blood) sample analysis. GMCS also can be applied as an efficient separation and preconcentration nanoprobe for surface assisted laser desorption/ionization (SALDI) and enhances the ionization of bacterial biomolecules during MALDI-MS analysis. The bacterial cell suspension was concentrated from 1 mL to 10 μL *via* an external magnetic field, thus it can enhance bacteria detection for MALDI-MS analysis. GMCS is an outstanding approach which is a rapid, sensitive, culture free technique and low cost biosensor for pathogenic bacteria detection.

Introduction

Graphene is a novel allotropic member of carbon-based nanomaterials with honeycomb structure.[1] It has attracted worldwide interest and the pioneer inventors have been awarded the Nobel Prize in physics in 2010.[1] Graphene has tremendous bioapplications due to excellent features such as high specific surface area, electronic conductivity, thermal conductivity, mechanical strength, cheap and easy to undergo functionalization *via* π–π interactions, covalent bonding, polymer blending and electrostatic interactions.[2–4] The achievements reported in the last three years have been reviewed by Jiang,[2] Guo and Dong,[3] Chhowalla *et al.*,[5] Liu and Feng,[6] Liu *et al.*,[7] Zhang *et al.*,[8] Cai *et al.*,[9] Lee *et al.*,[10] Lin *et al.*,[11] Chen *et al.*,[12] Pumera[13] and Lin *et al.*[14] Graphene has been used extensively for biosensing[2,10,13–23] and fluorescence imaging.[24–27] Chitosan (CS) is a natural biocompatible, biodegradable, and high mechanical strength biopolymer. The intrinsic biocompatibility, tensile strength, Young's modulus and adsorption of the graphene-based materials[28–31] and magnetic nanoparticles[32] are significantly improved by surface capping with chitosan.[28–32] Graphene has been demonstrated to have great potentials in electrical biosensing for single bacterium detection.[33]

Presence of pathogenic bacteria in blood is a serious health problem (*e.g.*, causing septic shock) because the recipients of blood transfusions are usually critically sick, which results in serious suppression of immunity. The growth rate of bacterial

[a]*Department of Chemistry, National Sun Yat-Sen University, Kaohsiung, 80424, Taiwan. E-mail: hwu@faculty.nsysu.edu.tw; Fax: +886-7-525-3908; Tel: +886-7-5252000-3955*

[b]*School of Pharmacy, College of Pharmacy, Kaohsiung Medical University, Kaohsiung, 806, Taiwan*

[c]*Center for Nanoscience and Nanotechnology, National Sun Yat-Sen University, Kaohsiung, 80424, Taiwan*

[d]*Doctoral Degree Program in Marine Biotechnology, National Sun Yat-Sen University, Kaohsiung, 80424, Taiwan*

† Electronic supplementary information (ESI) available. See DOI: 10.1039/c3tb20413h

contamination increases with time during storage (37 °C).[34] Therefore, it is extremely necessary to monitor the presence of bacteria in blood before a recipient's transfusion at low bacteria cell number. The detection of bacteria in blood suffers many challenges such as interferences of various biomolecules, such as albumin (major content 55–80%), salts, or blood cells. In order to improve the selectivity of the biosensor, unwanted protein signals must be removed. The detection of pathogenic bacteria plays a key role in the prevention and identification of problems related to human health and safety. Traditional methods used for bacteria detection may take up to 7–8 days.[35–37] Fluorescence microscopy exhibits some limitations such as; cell autofluorescence that can mask signals from the labeled molecules, requires a long waiting period and labeled biomolecules can undergo photobleaching.[38] However immuno-magnetic separation using magnetic nanoparticles coated with an antibody or quantum dots coated with an antibody is selective, but it is expensive, inhibits the cell growth, shows fluorescence peak shifts, is pH dependent, changes the size of nanoparticles due to aggregation, not very robust and time consuming.[39–45] Because today the biosensing research is growing rapidly, so it becomes critical to develop faster and more sensitive detection technologies.[46]

Graphene magnetic nanoparticles have been investigated in the literature.[30,47–52] The stability of magnetic nanoparticles increases when combined with a graphene nanosheet that shows high adsorption for the Fe_3O_4 core due to its large surface area. Therefore, magnetic nanoparticles prevent van der Waals forces which can cause irreversible graphene aggregation. These factors increase the material applicability in harsh conditions to be a long-term material.[53] Graphene-nanomagnetic hybrid materials are biocompatible.[46,53,54] Preparation of multifunctional graphene oxide-magnetic nanoparticles and their applications for drug delivery[55] and multifunctional applications of graphene for imaging experiments[56] have been reported. Recently, our group reported chitosan nanomagnets which were used to extract endotoxin of pathogenic bacteria from human urine samples.[57]

Herein, graphene-magnetic nanoparticles@chitosan (GMCS) is prepared and characterized to serve as biomedical and multi-functional biosensors based on the combination of magnetic nanoparticles and graphene properties. This biomaterial is proposed in order to achieve rapid, sensitive, and low cost detection of pathogenic bacteria (*Pseudomonas aeruginosa* and *Staphylococcus aureus*) in aqueous suspension and mouse blood samples. Fluorescence spectra show a linear relationship with low detection limits for both pathogenic bacteria. The bacteria which were separated from aqueous and blood samples prior to MALDI-MS analysis show enhancement of bacteria biomarker peaks. Both bacteria exhibit high affinity towards GMCS. We successfully integrated MALDI-MS (a qualitative technique) with fluorescence (a quantitative technique) for pathogenic bacteria detection.

Experimental section

Materials and instrumental conditions are discussed in detail in the ESI.†

Bacterial culture

Caution: Because the bacteria are pathogenic (class II), handling of the two bacteria must be done with care; wearing gloves and masks are requested for all experiments.

Both bacteria *S. aureus* (BCRC 10451) and *P. aeruginosa* (BCRC 10303) were cultivated at 37 °C and maintained on DifcoTM Nutrient Agar plates as shown in the ESI.† Bacteria colony number was evaluated by using the plate count protocol and the procedure details are described in the ESI.†

Preparation of graphene oxide (GO) and graphene colloid (G)

The oxidation of natural graphite to graphene oxide was performed from the modified method of Hummers;[58,59] the method was based on strong oxidation of graphite by $KMnO_4$ in strong acid, then further reduction using hydrazine as shown in Fig. 1A.

Preparation of magnetic nanoparticles capped with chitosan

The synthesis of the magnetic nanoparticles was modified from the procedures described in the literature,[60] which is based on the co-precipitation of ferrous and ferric salts as described in the ESI.† The percentage yields of chitosan immobilized on magnetic nanoparticles were calculated from the weight of dried nanoparticles after separation using an external magnetic field. The percentage of chitosan modified onto the magnetic nanoparticle surfaces was calculated based on the dry weight difference and it was about 3.0%.

Synthesis of graphene-magnetic@chitosan (GMCS)

About 1.0 g of graphene@chitosan was mixed with 1.0 g of Fe_3O_4@chitosan for 2 h. The product was separated by an external magnetic field and washed several times prior to use. The percentage yields of chitosan nanoparticles on graphene were calculated from the weight of dried nanoparticles. The amount of chitosan immobilized onto the graphene was 20%, thus the total amount of chitosan which was loaded onto the GMCS was 23% (wt/wt).

Sample preparation for fluorescence analysis

For detection of bacteria, suspension solutions with different concentrations (5.0×10^2, 1.0×10^3, 1.5×10^3, 2.0×10^3, 2.5×10^3, 3.0×10^3, 3.5×10^3, 4.0×10^3, and 4.5×10^3 cfu mL^{-1}) of *P. aeruginosa* and *S. aureus* (4.0×10^2, 9.0×10^2, 1.8×10^3, 2.2×10^3, 2.7×10^3, 3.1×10^3, 4.5×10^3, 4.9×10^3 cfu mL^{-1}) were prepared. To the above suspension solutions, about 0.25 μg (10 μL) of graphene-magnetic@chitosan (GMCS) was dispersed and incubated (1 min) before measurements. High cell numbers of pathogenic bacteria (1.0×10^5, 1.0×10^4 for *P. aeruginosa* and *S. aureus*, respectively) display rapid and spontaneous aggregation, as shown in the inset photograph of Scheme 1A. The control sample was performed from GMCS without the presence of any bacteria cells.

For detection of bacteria in blood, the mouse blood samples were diluted with deionized water fifty times before use. Different cell concentrations (5.0×10^2, 1.0×10^3, 1.5×10^3,

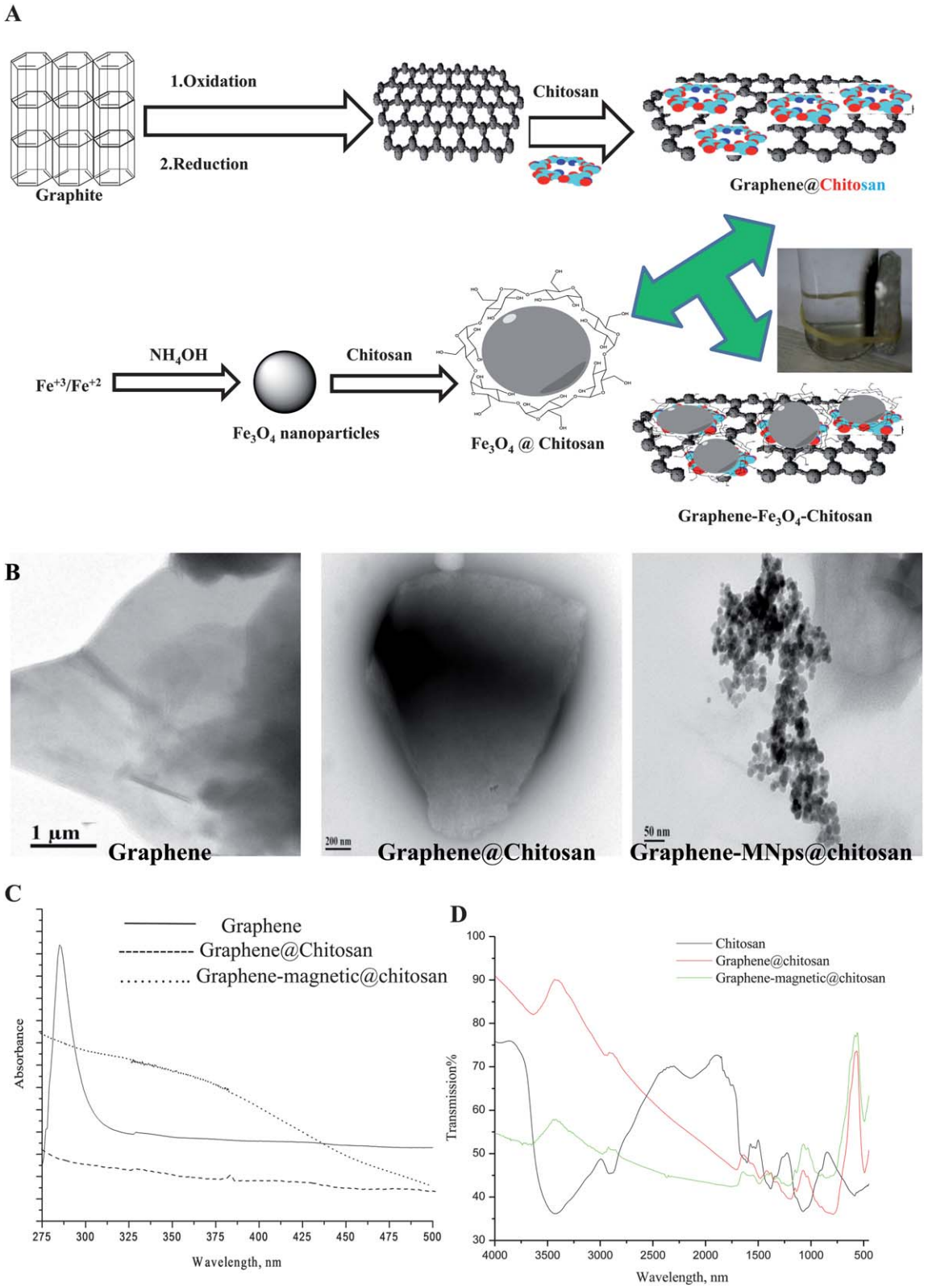

Fig. 1 (A) Schematic presentation of graphene-magnetic@chitosan preparation of graphene starting from graphite *via* oxidation/reduction, magnetic nanoparticles *via* coprecipitation, and graphene-magnetic nanoparticles capped with chitosan *via* the combination of graphene@chitosan and magnetic@chitosan, (B) TEM micrographs of graphene, graphene modified chitosan, and graphene-magnetic@chitosan, respectively, (C) UV spectra, and (D) FTIR spectra of chitosan, graphene@chitosan and graphene-magnetic@chitosan.

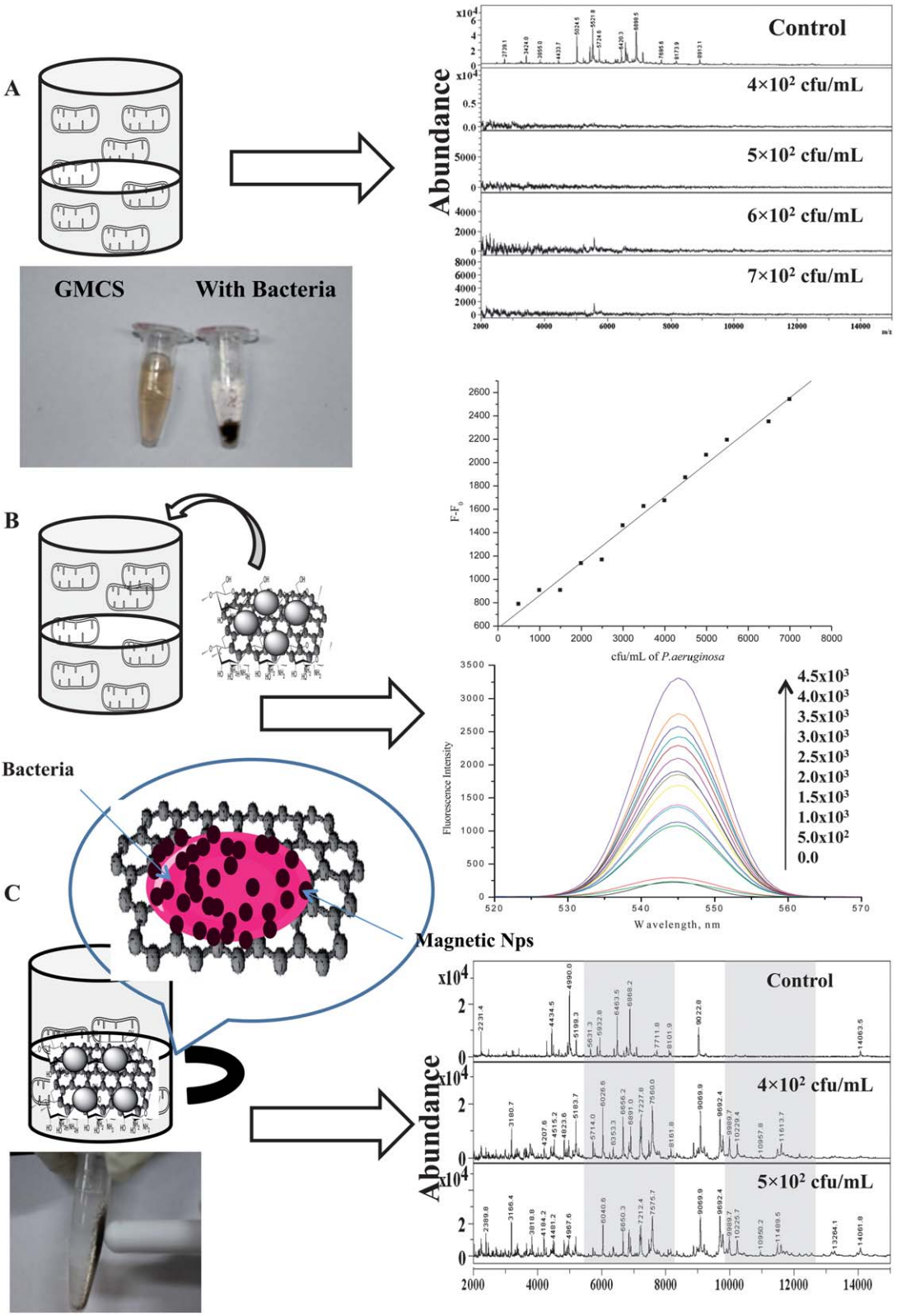

Scheme 1 Flow chart of the analysis procedure; (A) direct analysis using MALDI-MS of bacteria at low concentration, inset photograph represent GMCS with and without bacteria at high concentration, which shows aggregation in right hand sample, (B) direct analysis using fluorescence spectroscopy, and (C) separation and detection of the bacteria using MALDI-MS. Inset: photograph represents magnetic feature of GMCS-bacteria under an external magnetic field.

2.0×10^3, 2.5×10^3, 3.0×10^3, 3.5×10^3, 4.0×10^3, and 4.5×10^3 cfu mL^{-1}) of the two bacteria were added to 1.0 mL of blood samples, and then the fluorescence spectra were recorded. After that, 0.25 μg (10 μL) of GMCS was suspended in each solution and the fluorescence emission spectra were recorded directly, after incubation (1 min), as shown in Scheme 1B.

Separation and sample preparation for MALDI-TOF-MS analysis

About 0.25 μg (10 μL) of GMCS was suspended in 1.0 mL of water suspension containing different cell numbers of each bacteria (*P. aeruginosa* and *S. aureus*). High cell numbers of pathogenic bacteria (1.0×10^5 and 1.0×10^4 for *P. aeruginosa* and *S. aureus*, respectively) undergo rapid and spontaneous aggregation, so they were used directly for MALDI-MS analysis as shown in the photograph of Scheme 1A. The aggregation is due to the high affinity of bacteria towards GMCS surfaces. For low bacteria colony numbers (5.0×10^2, 1.0×10^3, 1.5×10^3, 2.0×10^3, 2.5×10^3, 3.0×10^3, 3.5×10^3, 4.0×10^3, and 4.5×10^3 cfu mL^{-1}) of *P. aeruginosa* and *S. aureus* (4.0×10^2, 9.0×10^2, 1.8×10^3, 2.2×10^3, 2.7×10^3, 3.1×10^3, 4.5×10^3, 4.9×10^3 cfu mL^{-1}), after 10 min, the GMCS was separated from the original bacteria suspension (1 mL) using an external magnetic field. The separated materials were diluted with 10.0 μL of sinapinic acid matrix solution (50.0 mM in aqueous acetonitrile (50 : 50)). About 2.0 μL of the mixture was spotted onto the MALDI plate, air dried and then subjected to MALDI-MS analysis.

Replication of batch experiments

Each experiment was conducted in triplicate to confirm the reproducibility. For gross error measurements, more repeats of experiments were performed according to the rejection of outliers from statistic treatment of data. The results presented with error bars are from the average of three repeated measurements from the same bacteria suspensions.

Results and discussion

Characterization of graphene-magnetic nanoparticles (Fe_3O_4) @chitosan (GMCS)

Although the preparation of monolayer graphene *via* mechanical exfoliation of graphite can produce graphene with high quality,[1] the yield of this technique is extremely low and the process is difficult to control. Thus, we followed Hummer's method which is based on an intensive oxidation of graphite using sulfuric acid and potassium permanganate (oxidizing agent) to produce graphene oxide (GO).[58] Graphene oxide was reduced by hydrazine (NH_2NH_2) to graphene as presented in Fig. 1A. The prepared graphene was functionalized with chitosan and then further modified with magnetic nanoparticles (Fig. 1A). Fig. S1A, ESI,† displays the FTIR spectra of graphene and graphene oxide. The intense bands at 3450 and 1250 cm^{-1} are attributed to the stretching of the O–H and of C–O, respectively. The band at 1650 cm^{-1} is associated with stretching of the C═O bond of carboxyl groups. The FTIR spectrum (Fig. S1A†) confirms the two step oxidation–reduction process of graphene, due to absence of the carbonyl group (C═O). Raman spectroscopy is a powerful, nondestructive tool which is applied to characterize carbon-based nanomaterials such as graphene. The Raman spectrum of graphene is plotted in Fig. S1B, ESI.† Generally, the Raman spectrum of graphene comprises three main distinctive peaks which are the diamondoid (D, 1350 cm^{-1}), graphitic (G, 1560 cm^{-1}) and 2D bands (2500 cm^{-1}). The diamondoid peak (D-band, 1350 cm^{-1}) is not always well observed; whereas the G-band was observed at 1560 cm^{-1} for the pristine graphene (G). Representative transmission electron microscopy (TEM) micrographs of the obtained graphene, graphene@chitosan and graphene-Fe_3O_4@chitosan (GMCS) nanohybrids are shown in Fig. 1B. Almost single or few layers of graphene sheets can be obtained by chemical synthesis from graphite (as indicated by the transparency of graphene sheet in the TEM image in Fig. 1B).[59] It can be seen that Fe_3O_4 nanoparticles have been coated onto the graphene surfaces and their loading amount was sufficient enough in order to exhibit the magnetic properties as shown in the inset camera photograph of Fig. 1A. Scanning electron microscopy image (SEM, Fig. S1C†) shows the rupture of graphene layers under the microscopy electron field. Graphene displays UV absorption at 270 nm (Fig. 1C).[59] The change in absorption pattern indicates successful modification of graphene by the chitosan and magnetic nanoparticles (Fig. 1C). Fourier transform infrared (FTIR) spectra were carried out to investigate the interactions among graphene, magnetic nanoparticles and chitosan. The FTIR spectrum (Fig. 1D) of pure chitosan offers an intense peak at 1588 cm^{-1}, corresponding to the amide II band; while the peaks at 1074 and 3450 cm^{-1} could be due to the –C–O–C– vibration and O–H stretching, respectively. The vibration bands of chitosan were shifted after interaction with graphene. For instance, O–H, amide II, –C–O–C– shifted to 3650, 1700, and 1200 cm^{-1}, respectively. The oxygen-containing groups and negative charges on the graphene surface can interact effectively with the polycationic chitosan through hydrogen bonding and electrostatic attractions.[28] Fluorescence spectra (Fig. 2A) of graphene, graphene@chitosan and graphene-magnetic nanoparticles@chitosan at the same excitation wavelength (270 nm) indicate no peak shifts in the graphene fluorophore. The latter observation implies that the magnetic nanoparticles play no effect in the fluorescence emission of graphene nanosheets. The crystalline structures of the prepared materials (pure Fe_3O_4, graphite, and GMCS) were investigated with X-ray diffraction (XRD, Fig. S1D†). Six characteristic peaks for Fe_3O_4 ($2\theta = 30.1$, 35.5, 43.3, 53.4, 62.51 and 73.95), identified by their indices ((220), (311), (400), (422), (440) and (553)) were observed in the samples (Fig. S1D†). These results are consistent with the standard XRD data for the inverse spinel structure of Fe_3O_4 (JCPDS file no. 19-0629). In the case of GMCS, a broad diffraction peak at $2\theta = 20.0$ belongs to the (001) crystal phase of graphene. Pristine graphite can be recognized from a peak at $2\theta = 28.00$ corresponding to (002). The amount of chitosan which immobilized onto the GMCS was calculated. According to the preparation procedures, chitosan was divided between two sources, *i.e.* magnetic nanoparticles (Fe_3O_4) and graphene

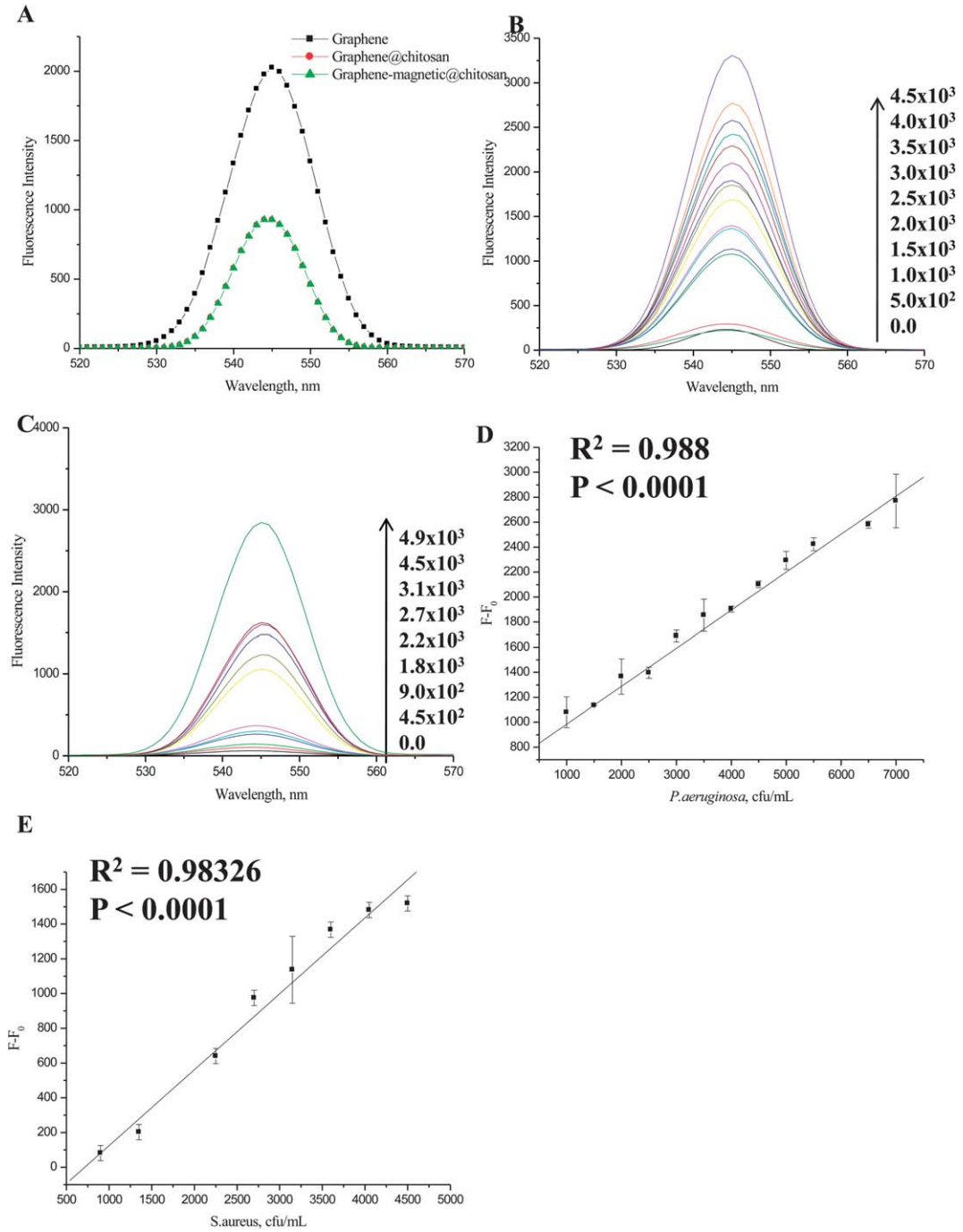

Fig. 2 (A) Fluorescence emission spectra of graphene, graphene@chitosan and graphene-magnetic@chitosan, fluorescence emission with different colony units of (B) *P. aeuginosa*, and (C) *S. aureus* which give a linear relationship of (D) *P. aeruginosa* and (E) *S. aureus*.

nanosheet. The calculated percentage of chitosan on magnetic nanoparticles was 3%, while on the graphene sheet it was 20%. The immobilization of a higher concentration of chitosan to the graphene nanosheet than magnetic nanoparticles is due to the high surface area, roughness, zeta potential[43] and hydrophobic interaction with graphene which assists more chitosan to immobilize effectively to the surface. Thus, the total chitosan immobilized onto the GMCS was 23%. From the fluorescence calibration curve (Fig. S1E†) of GMCS and dried weight calculation, the percentage of magnetic nanoparticles was 20% which is in agreement with the literature which used atomic absorption spectroscopy (AAS).[61]

The overall process of GMCS for biosensing of bacteria using fluorescence spectroscopy and MALDI-MS are schematically summarized in Scheme 1. Scheme 1 presents three different procedures to detect the bacteria suspension. By using direct MALDI-MS analysis of low bacteria concentration shows no detection of any bacteria cells (Scheme 1A) due to low biomolecules content. When GMCS was added to the bacteria suspension, direct measurements of fluorescence were

successfully recorded with linear relationship (Scheme 1B). Based on the magnetic properties and high affinity of bacteria to aggregate on nanocomposite surface (inset photography of Scheme 1A, at high concentration), bacteria can be separated without external magnets. At low concentration, bacteria were separated by external magnets and concentrated from 1 mL to 10 μL. Due to large surface area and small bacteria volume, suspension solution which display no peaks (Scheme 1A), can be successfully detected (Scheme 1C). Furthermore, MALDI-MS signals of bacteria cells can be significantly improved.

Fluorescence biosensing of pathogenic bacteria suspension by using the GMCS approach

Detection of a low number of bacteria cells represents the ultimate level of sensitivity and has been a longstanding goal of analytical methods. The fluorescence biosensing depends on the use of a nanoprobe (GMCS) that changes intensity in response to a change in bacteria cell number.[44] Because fluorescence is high sensitivity, and also due to a bright signal appearing against a dark background, it is an excellent technique for bacteria detection and better than other spectroscopy methods, such as the UV absorption method. However, direct bacteria detection using fluorescence would be a difficult task, particularly in complex biological samples due to biomolecule interferences, such as proteins, which can display intrinsic fluorescence (aromatic amino acid). In any real sample detection system such as bacteria samples, there will be background signals due to impurities in the samples, emission from optical components, scattered light at the incident wavelength, and dark current from the detector. Thus, a reference fluorophore is necessary to delete all or some of these factors. The intrinsic fluorescence of cell biomolecules would further complicate the fluorescence spectra. For instance, we have to deal with multiple fluorophores which undergo overlapping among the absorption and emission spectra. In most of the conventional techniques, the accurate bacteria cell number can only be obtained after the bacteria crops are cultured; hence, the adjustment of parameters depends solely on experience and large amounts of experiments. They need at least 2–8 days to obtain a confirmed result.[34–36] Also, the sensitivity is typically poor. Thus, it is important to develop an effective biosensor that can generate photoluminescence as a function of the bacteria cells number. As shown in Fig. 2B (*P. aeruginosa*) and Fig. 2C (*S. aureus*), there is an increase in fluorescence intensity with increase in the concentration of colony forming units (cfu mL^{-1}). Graphene works intrinsically as a quencher for bacteria autofluorescence as it has a long life time. The increase in intensities for the various numbers of bacteria cells are thought to be due to different parameters such as aggregation of bacteria onto the surfaces of GMCS. This aggregation can be observed by the naked eye at high concentration or long incubation time as shown in the inset photograph of Scheme 1A. There is a good linear relationship between the difference of fluorescence intensity in the presence "F" and absence "F_0" of pathogenic bacteria *i.e. P. aeruginosa* (Fig. 2D) and *S. aureus* (Fig. 2E).

When high numbers of bacteria cells (1×10^5 and 1×10^4 cfu mL^{-1} for *P. aeruginosa* and *S. aureus*, respectively) were investigated, direct aggregation and sedimentation of bacteria have been observed as shown in the photographic image of Scheme 1A. Thus low cell numbers have been demonstrated here. The latter observation indicates the high affinity of GMCS to both bacteria. The aggregation is due to accumulation of bacteria cells onto the surfaces of nanocomposite GMCS. The new composite (bacteria and GMCS) becomes heavy so it was sedimented. Limits of detection of the two bacteria in water are 5.0×10^2 and 4.5×10^2 cfu mL^{-1}, respectively. All analytical parameters are tabulated in Table 1.

Matrix assisted laser desorption/ionization mass spectrometry of standard bacteria suspensions

MALDI mass spectrometry has been used as a fast technique applied to bacteria analysis.[62–68] Identification of the microorganism is easier when high numbers of bacteria biomarker were ionized and detected in the MALDI-MS spectra.[64] Bacteria are not simple compounds, or even mixtures of biomolecules. They are complex microorganisms and their biomolecules undergo many associations, thus the MALDI ionization/desorption processes are seriously influenced by the ion suppression effect. When GMCS was added to the bacteria suspension at high concentration, an aggregation with GMCS was observed which is due to the strong interactions as shown in the inset photograph of Scheme 1A. This sedimentation reveals the potential application of GMCS to purify water from bacteria and directly detect the bacteria without using an external magnetic field at high concentrations. Because biological samples typically have extremely low bacteria concentrations, we restrict the work to low concentrations of bacteria detection. Direct analysis of *P. aeruginosa* (Fig. S2(A)†) and *S. aureus* (Fig. S2(B)†) suspension solutions of low concentrations failed to identify the bacteria due to low biomolecule contents. However, detection can be successful when bacteria suspensions were preconcentrated from 1 mL to 10 μL using an external magnetic field as shown in Fig. 3A and B. *P. aeruginosa* (Fig. 3A) and *S. aureus* (Fig. 3B) show increases of biomarker peaks that enhance the discrimination between the microorganism after separation. These improvements are due to increased surface area *via* graphene and magnetic nanoparticles that work as a co-matrix with sinapinic acid *i.e.* surface assisted laser desorption/ionization mass spectrometry (SALDI-MS).[67,68] Furthermore, the separated bacteria-GMCS was suspended into the acidic matrix directly thus the cell

Table 1 Limit of detection of both bacteria using fluorescence and MALDI-MS

		P. aeruginosa (cfu mL^{-1})	*S. aureus* (cfu mL^{-1})
Fluorescence	Suspension	5.0×10^2	4.5×10^2
	Blood	4.0×10^2	1.0×10^2
MALDI	Suspension	5.0×10^2	4.5×10^2
	Blood	6.0×10^2	5.0×10^2

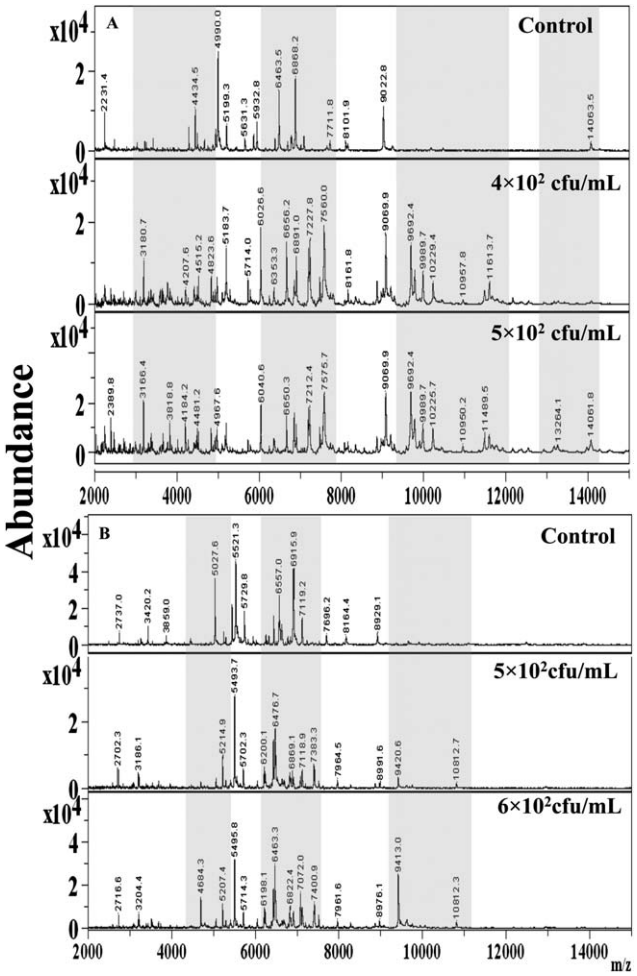

Fig. 3 MALDI spectra of bacteria suspension solution for (A) *P. aeruginosa* and (B) *S. aureus* after separation with different bacteria numbers, white highlight (darker 35%) represents the bacteria enhancement.

membranes undergo acidic hydrolysis. The limits of detection for both bacteria detected by the current approach are tabulated in Table 1.

Fluorescence biosensing of pathogenic bacteria in blood samples

Detection or quantification of bacteria in blood is a crucial challenge as albumin (that represents 55–80% of blood protein content), other proteins and blood cells display autofluorescence that masks bacterial autofluorescence, thus leading to overlapping. These biomolecules can exhibit interactions with bacteria cells. For instance, when different number of cells of *P. aeruginosa* (Fig. 4A) or *S. aureus* (Fig. 4B) were added to albumin fluorophore (blood sample), albumin fluorescence was quenched. This quenching may be due to the interactions with the bacteria cells with albumin serum or due to collisions. Graphene has a long fluorescence lifetime, thus it can reduce the autofluorescence of biological system in a manner similar to quantum dots.[2,5–12] Graphene has fluorescence lifetimes longer than autofluorescence, thus it can drastically reduce the signal of the common background which is emitted from the biological samples (Fig. 4C). Fluorescence upon addition of different cell numbers of *P. aeruginosa* (Fig. 4D) and *S. aureus* (Fig. 4E) to GMCS, fluorescence signals of GMCS was increased as in standard bacteria (Fig. 2B–E). The difference of fluorescence in the presence (F) and absence of bacteria (F_0) exhibits excellent linear relationships in the cases of *P. aeruginosa* (Fig. 4F) and *S. aureus* (Fig. 4G) with linear dynamic ranges of 4.0×10^2 to 4.0×10^3 and 1.0×10^2 to 3.0×10^3 cfu mL^{-1}, respectively. Additional background subtraction can substantially improve the signal-to-noise (S/N) ratios of the resulting spectra. The limits of detection of blood analyses are tabulated in Table 1. However, blood is a complicated sample with many metals, proteins, and cells; it is worth mentioning that these metals can bind to the chitosan backbone; enriched by coordinating ligands, and thus improve bacteria binding to GMCS.[59] Low limits of detection of both bacteria (Table 1) in the blood samples are due to the high salt contents of blood and antibodies that can cause the death of bacteria cells, and results in low cell counts. Furthermore, the metals coordinate with bacteria and GMCS and enhance non-covalent binding.

Forces governing the binding between bacteria and nano-hybrid (GMCS)

The interactions between the pathogenic bacteria with GMCS can explain the reason for fluorescence enhancement. The binding forces between bacteria cells and GMCS were based on two different sources; one is from graphene and the other is from chitosan. The two sources reinforce each other, *i.e.* complementary forces. The oxygen-containing groups, negative charges on the graphene surface and the polycationic chitosan (CS) can interact effectively with the bacteria *via* hydrogen bonding, hydrophobic and electrostatic interactions, acid–base interactions, π–π interactions and polar functional groups interactions.[67,69] From the above description, we can recognize that graphene-magnetic@chitosan (GMCS) is a multifunctional material that is assisted by different adsorption mechanisms. Due to these forces, GMCS offers high sensitivity in fluorescence analysis for blood samples. Zeta (ζ) potential measurements of graphene, chitosan, and graphene@chitosan were −46, +100, and +40 mV, respectively.[43] The negative ζ potential of graphene and the positive charge of the chitosan solution confirm the interactions were mainly electrostatic interactions. The ζ potential of the nanocomposite (graphene–chitosan) is greatly different from its parent suspensions[43] (*i.e.* +40 mV), which enhances the interaction between the negative charge of bacteria with the positive charge of GMCS. These factors assist bacterial cells to be entrapped with the chitosan matrix onto the surface of GMCS,[64] so that it can aggregate at high concentration. In addition, the two-dimensional GMCS sheet is equipped with many functional groups which can intensively interact with the pathogenic bacteria *via* non-covalent interactions. Thus, it provides the highest extraction efficiencies of bacteria biomolecules compared with other materials.

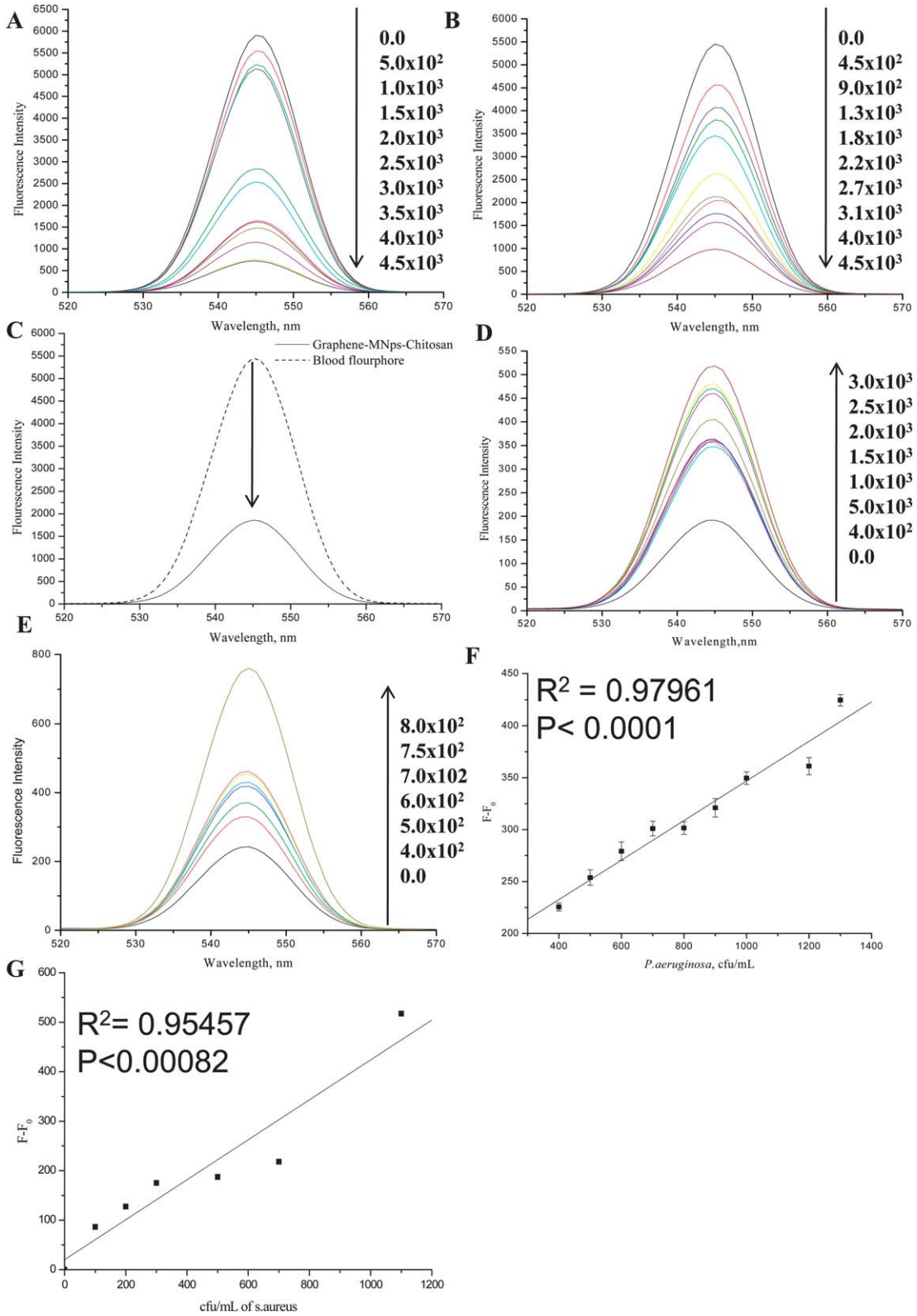

Fig. 4 Fluorescence analysis of blood samples. Effect of (A) *P. aeruginosa* and (B) *S. aureus* (B) on blood fluorophore (mainly albumin), (C) effect of graphene-magnetic@chitosan on blood fluorophore, fluorescence response of GMCS upon addition of (D) *P. aeruginosa* and (E) *S. aureus* and their linear relationships (F–G), respectively.

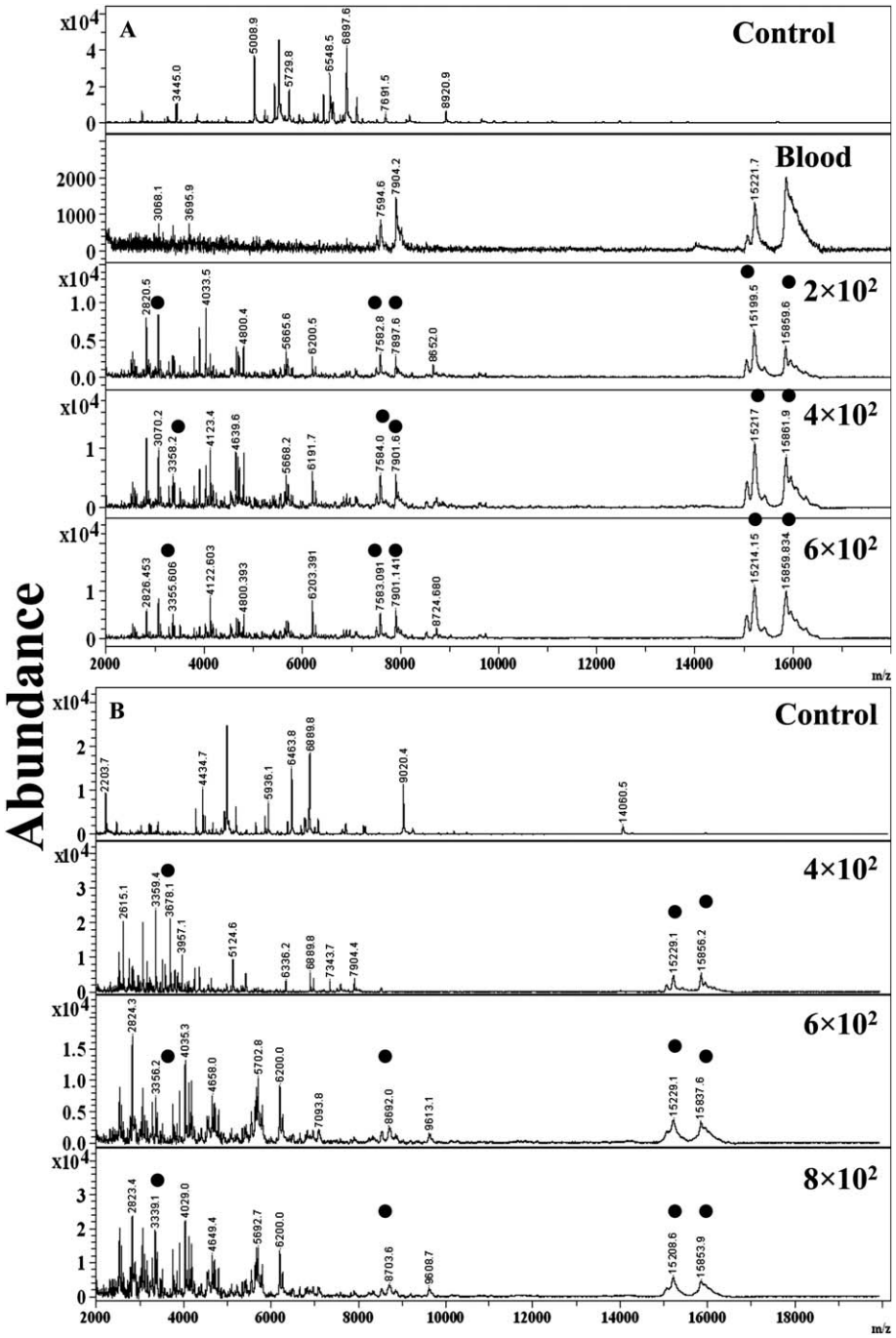

Fig. 5 MALDI spectra of blood samples for (A) *P. aeruginosa* and (B) *S. aureus* after separation with different concentrations, marks (●) represent biomolecules belonging to blood.

Matrix assisted laser desorption/ionization mass spectrometry analysis of bacteria from blood samples

Direct detection of pathogenic bacteria from blood samples using MALDI-MS suffers from ion suppression due to the existence of high concentrations of blood proteins and salts. Direct analysis of blood samples of *P. aeruginosa* (Fig. S3(A)†) and *S. aureus* (Fig. S3(B)†) at low concentrations present low or no biomolecule peaks that make bacteria discrimination a difficult task. Thus, unwanted protein signals and salts must be removed or cancelled. Separation of bacteria biomolecules by external magnets could reduce these interferences. MALDI-MS spectra of *S. aureus* (Fig. 5A) and *P. aeruginosa* (Fig. 5B) have demonstrated the applicability of GMCS to separate, preconcentrate and enhance bacteria proteins from blood samples with different colony forming units. The protein peaks of blood are represented by the solid black circle (●) and the rest of the peaks belong to bacteria biomolecules. It is worth mentioning that the introduced GMCS system shows good biocompatibility

as most of its constituents are intrinsically biocompatible.[70–77] Biocompatibility of graphene is increased after capping with chitosan as sharp edges and metal contents are decreased.[71–77] Graphene-magnetic@chitosan nanocomposite is capable of further applications in biology. Thermodynamic analysis of the interactions between chitosan and bacteria cells *via* quantum dots (CdS) modified chitosan[67] reveals the interactions between chitosan and bacteria are entropically driven and spontaneous. Data also reveal stronger interactions between chitosan and bacteria in the case of *S. aureus* than *P. aeruginosa* due to greater enrichment of the peptidoglycan content of the former than the latter. The strong interaction between chitosan to *S. aureus* is the primary reason why GMCS shows better sensitivity in the case of *S. aureus* than *P. aeruginosa*. Due to this binding affinity, *S. aureus* show aggregation even at low concentrations when incubated or vortexed for a long time.

Conclusion

Graphene-magnetic@chitosan (GMCS) displays a wide applicability to work as a rapid and sensitive biosensor for pathogenic bacteria for fluorescence spectroscopy and MALDI-MS. Background subtraction and quenching of autofluorescence could enhance fluorescence detection and offer also quantitative analysis. The nanohybrid (GMCS) biosensor offers many advantages such as excellent robustness, improved assay simplicity, and the capability for fluorescence based real-sample monitoring. The new nanobiosensor also shows good separation, preconcentration, co-matrix and could effectively enhance bacteria ionization during MALDI-MS analysis. The biocompatibility of GMCS is a promising feature for both *in vitro* and *in vivo* applications for biological and biomedicine studies in the near future.

Acknowledgements

We thank the National Science Council (NSC), Taiwan, for financial support. Hani Nasser Abdelhamid thanks the Chemistry Department, Assuit University, Egypt, for the permission of leave to study for the masters degree at the Department of Chemistry, National Sun Yat-Sen University to carry out this work.

References

1 K. S. Novoselov, A. K. Geim, S. V. Morozov, D. Jiang, Y. Zhang and S. V. Dubonos, *Science*, 2004, **306**, 666–669.
2 H. Jiang, *Small*, 2011, **7**, 2413–2427.
3 S. J. Guo and S. J. Dong, *Chem. Soc. Rev.*, 2011, **40**, 2644–2672.
4 S. Stankovich, D. A. Dikin, R. D. Piner, K. A. Kohlhaas, A. Kleinhammes and Y. Wu, *Carbon*, 2007, **45**, 1558–1565.
5 K. P. Loh, Q. Bao, G. Eda and M. Chhowalla, *Nature*, 2010, **2**, 1015–1024.
6 L. Z. Feng and Z. Liu, *Nanomedicine*, 2011, **6**, 317–324.
7 Z. Liu, J. T. Robinson, S. M. Tabakman, K. Yang and H. Dai, *Mater. Today*, 2011, **14**, 316–323.
8 H. Shen, L. Zhang, M. Liu and Z. Zhang, *Theranostics*, 2012, **2**, 283–294.
9 Y. Zhang, T. R. Nayak, H. Hong and W. Cai, *Nanoscale*, 2012, **4**, 3833–3842.
10 T. Kuila, S. Bose, P. Khanra, A. K. Mishra, N. H. Kim and J. H. Lee, *Biosens. Bioelectron.*, 2011, **26**, 4637–2648.
11 Y. Wang, Z. Li, J. Wang, J. Li and Y. Lin, *Trends Biotechnol.*, 2011, **29**, 205–212.
12 Y. Liu, X. Dong and P. Chen, *Chem. Soc. Rev.*, 2012, **41**, 2283–2307.
13 M. Pumera, *Mater. Today*, 2011, **14**, 308–315.
14 Y. Shao, J. Wang, H. Wu, J. Liu, I. A. Aksay and Y. Lin, *Electroanalysis*, 2010, **22**, 1027–1036.
15 S. Mao, G. Lu, K. Yu, Z. Bo and J. Chen, *Adv. Mater.*, 2010, **22**, 3521–3526.
16 F. Li, Y. Huang, Q. Yang, Z. Zhong, D. Li and L. Wang, *Nanoscale*, 2010, **2**, 1021–1026.
17 C. H. Lu, H. H. Yang, C. L. Zhu, X. Chen and G. N. Chen, *Angew. Chem.*, 2009, **121**, 4879–4881.
18 S. Alwarappan, C. Liu, A. Kumar and C.-Z. Li, *J. Phys. Chem. C*, 2009, **113**, 8853–8857.
19 S. Alwarappan, A. Erdem, C. Liu and C. Z. Li, *J. Phys. Chem. C*, 2010, **114**, 12920–12924.
20 S. Alwarappan, S. Boyapalle, A. Kumar, C.-Z. Li and S. Mohapatra, *J. Phys. Chem. C*, 2012, **116**, 6556–6559.
21 S. Alwarappan, S. R. Singh, S. Pillai, A. Kumar and S. Mohapatra, *Anal. Lett.*, 2012, **45**, 746–753.
22 J. Balapanuru, J.-X. Yang, S. Xiao, Q. Bao, M. Jahan, L. Polavarapu, J. Wei, Q.-H. Xu and K. P. Loh, *Angew. Chem.*, 2010, **122**, 6699–6703.
23 S. Alwarappan, K. Cissell, S. Dixit, C.-Z. Li and S. Mohapatra, *J. Electroanal. Chem.*, 2012, **686**, 69–72.
24 C. Peng, W. Hu, Y. Zhou, C. Fan and Q. Huang, *Small*, 2010, **6**, 1686–1692.
25 M. L. Chen, J. W. Liu, B. Hu and J. H. Wang, *Analyst*, 2011, **136**, 4277–4283.
26 C. Guo, B. Book-Newell and J. Irudayaraj, *Chem. Commun.*, 2011, **47**, 12658–12660.
27 S. H. Hu, Y. W. Chen, W. T. Hung, I. W. Chen and S. Y. Chen, *Adv. Mater.*, 2012, **24**, 1748–1754.
28 X. Yang, Y. Tu, L. Li, S. Shang and X. M. Tao, *ACS Appl. Mater. Interfaces*, 2010, **2**, 1707–1713.
29 H. Bao, Y. Pan, Y. Ping, N. G. Sahoo, T. Wu and J. Li, *Small*, 2011, **7**, 1569–1578.
30 H. Fan, L. Wang, K. Zhao, N. Li, Z. Shi and Z. Ge, *Biomacromolecules*, 2010, **11**, 2345–2351.
31 L. Fan, C. Luo, X. Li, F. Lu, H. Qiu and M. Sun, *J. Hazard. Mater.*, 2012, **215**, 272–279.
32 Y. Y. Liang and L. M. Zhang, *Biomacromolecules*, 2007, **8**, 1480–1486.
33 N. Mohanty and V. Berry, *Nano Lett.*, 2008, **8**, 4469–4476.
34 (*a*) H. G. Braine, T. S. Kickler, P. Charache, P. M. Ness, J. Davis, C. Reichart and A. K. Fuller, *Transfusion*, 1986, **26**, 391–393; (*b*) S. J. Wagner, L. I. Friedman and R. Y. Dodd, *Clin. Microbiol. Rev.*, 1994, **7**, 290–302; (*c*) K. C. Anderson, M. A. Lew, C. Gorgone, J. Martel, C. B. Leamy and B. Sullivan, *Am. J. Med.*, 1986, **81**, 405–411.

35 O. Lazcka, F. J. Del Campob and F. X. Muñoz, *Biosens. Bioelectron.*, 2007, **22**, 1205–1217.
36 K. Levi, J. Smedley and K. J. Towner, *Clin. Microbiol. Infect.*, 2003, **9**, 754–758.
37 D. Ivnitski, I. Abdel-Hamid, P. Atanasov and E. Wilkins, *Biosens. Bioelectron.*, 1999, **14**, 599–624.
38 X. Michalet, F. F. Pinaud, L. A. Bentolila, J. M. Tsay, S. Doose and J. J. Li, *Science*, 2005, **307**, 538–544.
39 H. Gu, P. L. Ho, K. W. Tsang, L. Wang and B. Xu, *J. Am. Chem. Soc.*, 2003, **125**, 15702–15703.
40 A. J. Kell, G. Stewart, S. Ryan, R. Peytavi, M. Boissinot and A. Huletsky, *ACS Nano*, 2008, **2**, 1777–1788.
41 J. Gao, L. Li, P. L. Ho, G. C. Mak, H. Gu and B. Xu, *Adv. Mater.*, 2006, **18**, 3145–3148.
42 K. El-Boubbou, C. Gruden and X. Huang, *J. Am. Chem. Soc.*, 2007, **129**, 13392–13393.
43 S. Ryan, A. J. Kell, H. Van Faassen, L. L. Tay, B. Simard and R. MacKenzie, *Bioconjugate Chem.*, 2009, **20**, 1966–1974.
44 L. Bromberg, F. P. Chang, C. Alvarez-Lorenzo, B. Magarinos, A. Concheiro and T. A. Hatton, *Langmuir*, 2010, **26**, 8829–8835.
45 X. Xue, I. Pan, H. Xie, J. Wang and S. Zhang, *Talanta*, 2009, **77**, 1808–1813.
46 A. P. F. Turner, Biosensors, in *McGraw-Hill Yearbook of Science & Technology 2000*, McGraw-Hill, New York, 1999, pp. 39–42.
47 X. Y. Yang, X. Y. Zhang, Y. F. Ma, Y. Huang, Y. S. Wang and Y. S. Chen, *J. Mater. Chem.*, 2009, **19**, 2710–2714.
48 H. P. Cong, J. J. He, Y. Lu and S. H. Yu, *Small*, 2010, **6**, 169–173.
49 Q. F. Liu, W. C. Ren, Z. G. Chen, B. L. Liu, B. Yu and F. Li, *Carbon*, 2008, **46**, 1417–1423.
50 T. Szabo, A. Bakandritsos, V. Tzitzios, E. Devlin, D. Petridis and I. Dekany, *J. Phys. Chem. B*, 2008, **112**, 14461–14469.
51 F. He, J. Fan, D. Ma, L. Zhang, C. Leung and H. L. Chan, *Carbon*, 2010, **48**, 3139–3144.
52 G. Zhao, S. Song, C. Wang, Q. Wu and Z. Wang, *Anal. Chim. Acta*, 2011, **708**, 155–159.
53 Q. Liu, J. Shi and G. Jiang, *TrAC, Trends Anal. Chem.*, 2012, **37**, 1–8.
54 K. Liu, J. J. Zhang, F. F. Cheng, T. T. Zheng, C. Wang and J. J. Zhu, *J. Mater. Chem.*, 2011, **21**, 12034–12040.
55 L. Chang, S. Chen, P. Jin and X. Li, *J. Colloid Interface Sci.*, 2012, **388**, 9–14.
56 G. Gollavelli and Y. C. Ling, *Biomaterials*, 2012, **33**, 2532–2545.
57 J. Gopal, H. N. Abdelhamid, P.-Y. Hua and H. F. Wu, *J. Mater. Chem. B*, 2013, **1**, 2463–2475.
58 W. S. Hummers and R. E. Offeman, *J. Am. Chem. Soc.*, 1958, **80**, 1339.
59 H. N. Abdelhamid and H. F. Wu, *Anal. Chim. Acta*, 2012, **751**, 94–104.
60 D. Dorniani, M. Zobir, B. Hussein, A. U. Kura, S. Fakurazi, A. H. Shaari and Z. Ahmad, *Int. J. Nanomed.*, 2012, **7**, 5745–5756.
61 X. Yang, X. Zhang, Y. Ma, Y. Huang, Y. Wang and Y. Chen, *J. Mater. Chem.*, 2009, **19**, 2710–2714.
62 J. Gopal, C. H. Lee and H. F. Wu, *J. Proteomics*, 2012, **75**, 2972–2982.
63 M. A. Claydon, S. N. Davey, V. Edwards-Jones and D. B. Gordon, *Nat. Biotechnol.*, 1996, **14**, 1584–1586.
64 C. Fenselau, V. Ryzhov, Y. P. Ho and P. A. Demirev, *Anal. Chem.*, 1999, **71**, 2732–2738.
65 H. N. Abdelhamid, J. Gopal and H.-F. Wu, *Anal. Chim. Acta*, 2013, **767**, 104–111.
66 H. F. Wu, J. Gopal, H. N. Abdelhamid and N. Hasan, *Proteomics*, 2012, **12**, 2949–2961.
67 H. N. Abdelhamid and H. F. Wu, *J. Mater. Chem. B,* submitted.
68 X. Dong, J. Cheng, J. Li and Y. Wang, *Anal. Chem.*, 2010, **82**, 6208–6214.
69 Y. Liu, J. Y. Liu, C. H. Deng and X. M. Zhang, *Rapid Commun. Mass Spectrom.*, 2010, **25**, 3223–3234.
70 W. P. Xu, L. C. Zhang, J. P. Li, Y. Lu, H. H. Li and Y. N. Ma, *J. Mater. Chem.*, 2011, **21**, 4593–4597.
71 D. Odaci, S. Timur and A. Telefoncu, *Sens. Actuators, B*, 2008, **134**, 89–94.
72 H. L. Fan, L. L. Wang, K. K. Zhao, N. Li, Z. J. Shi and Z. G. Ge, *Biomacromolecules*, 2010, **11**, 2345–2351.
73 T. R. Nayak, H. Andersen, V. S. Makam, C. Khaw, S. Bae and X. Xu, *ACS Nano*, 2011, **5**, 4670–4678.
74 W. Hu, C. Peng, W. Luo, M. Lv, X. Li and D. Li, *ACS Nano*, 2010, **4**, 4317–4323.
75 T. Mondal, A. K. Bhowmick and R. Krishnamoorti, *J. Mater. Chem.*, 2012, **22**, 22481.
76 O. Akhavan and E. Ghaderi, *ACS Nano*, 2010, **4**, 5731–5736.
77 H. N. Lim, N. M. Huang and C. H. Loo, *J. Non-Cryst. Solids*, 2012, **358**, 525–530.